

Dye-sensitized solar cells based on dyes extracted from dried plant leaves

Sofyan A. TAYA^{1,*}, Taher M. EL-AGEZ¹, Kamal S. ELREFI¹,
Monzir S. ABDEL-LATIF²

¹Physics Department, Islamic University of Gaza, Gaza, Palestinian Authority

²Chemistry Department, Islamic University of Gaza, Gaza, Palestinian Authority

Received: 31.12.2013 • Accepted: 19.08.2014 • Published Online: 23.02.2015 • Printed: 20.03.2015

Abstract: In this work, natural dyes were extracted from dried plant leaves of plant cream, apricot, figs, apples, sage, thyme, mint, *Ziziphus jujuba*, orange, shade tree, basil, berry, Mirabelle plum, Victoria plum, peach, mango, pomegranate, banana, guava, and fluoridation-treated plant. The extracts were used as photosensitizers for dye-sensitized solar cells (DSSCs). The cells were assembled using nanostructured TiO₂ films. The best performance was observed for the DSSC sensitized with *Ziziphus jujuba* with an efficiency of 1.077%. The impedance spectroscopy of 3 cells was carried out and the equivalent circuits were found.

Key words: Dye-sensitized solar cells, natural dyes, plant leaves

1. Introduction

Since the pioneering work of O'Regan and Grätzel in 1991 [1], great attention has been directed to dye-sensitized solar cells (DSSCs) as cheap, effective, and environmentally benign candidates for a new generation of solar power devices [2–13]. A DSSC is a photoelectrochemical device that effectively converts sunlight into electricity. Generally, a DSSC consists of a fluorine-doped SnO₂ (FTO) layer, a nanocrystalline wide band-gap metal oxide semiconductor porous electrode, dye, an electrolyte, and a counter electrode. When a DSSC is illuminated with sunlight, the dye absorbs incident light and becomes excited. The absorption of light by the dye is followed by the injection of an electron from the lowest unoccupied molecular orbital (LUMO) level of the excited dye to the conduction band of the semiconductor. Simultaneously, the oxidized dye is reduced by the electron donor in the electrolyte and returns to the ground state. The electrons in the conduction band of the semiconductor flow through the external circuit toward the counter electrode, which regenerates the redox electrolyte. Through these processes, radiant energy is converted into electricity. Optimization of a DSSC is still a challenging task, as it is a highly complex interacting molecular system. Surface-adsorbed species exert a profound influence on the efficiency of a DSSC. Furthermore, the interfacial ion concentration also affects the stability of sensitizer surface attachment.

The use of natural pigments as sensitizing dyes for the conversion of solar energy into electricity is very interesting because they enhance the economical aspect and also have significant environmental benefits. Natural pigments extracted from fruits and vegetables, such as chlorophyll, have been extensively investigated as DSSC sensitizers [7–13].

The conversion efficiency is determined by 2 main factors: 1) the maximum photocurrent density,

*Correspondence: staya@iugaza.edu.ps

called the short circuit current density (J_{sc}), related to the charge injection rate from the dye LUMO to the semiconductor conduction bands; and 2) the open circuit voltage (V_{oc}). The highest efficiency of DSSCs was observed for cells sensitized by ruthenium complexes adsorbed on nanocrystalline TiO_2 , which reached 11%–12%, but they are still not suitable due to the high cost [6].

In this work, natural dyes were extracted from 20 dried plant leaves. These extracts were characterized by UV-Vis spectrophotometry. The photovoltaic properties of the fabricated DSSCs were investigated to determine the photoelectrochemical parameters of the cells. Moreover, 3 cells were examined by impedance spectroscopy (IS) since IS has become a major tool for investigating the properties and quality of DSSCs.

2. Experimental work

2.1. Preparation of natural dye sensitizers

Twenty plant leaves were collected from various plants and left to dry. The dried leaves were first washed with distilled water, then crushed into fine powder using a mortar. The powders were soaked in ethyl alcohol at room temperature in the dark for 1 day. After filtration of the solutions, natural dye extracts were obtained.

2.2. Preparation of dye-sensitized solar cells

FTO conductive plates with sheet resistance of $15 \Omega/cm^2$ and transmission $>80\%$ (Xinyan Tech. Ltd, Hong Kong) were cut into 1.6×1.6 cm pieces. The glass was cleaned in a detergent solution using an ultrasonic bath for 9 min, rinsed with water and ethanol, and then dried in an oven at $60^\circ C$ for 30 min. The TiO_2 paste was prepared by combining 50 mg of TiO_2 nanoparticles of 10–25 nm in size (US Research Nanomaterial Inc., USA) and 50 mg of polyethylene glycol, then grinding the mixture for 30 min until a homogeneous paste was obtained. Films of the prepared TiO_2 paste were deposited on the FTO surface by the doctor blade technique. After spreading the paste, the films were left to dry in an oven at $70^\circ C$ for 30 min. The films were then sintered at $450^\circ C$ for 40 min and were cooled down to about $70^\circ C$ [9,10]. The thickness of the sintered films was measured using an Olympus polarizing microscope BX53-P equipped with DP73 camera and it was found to be about $22 \mu m$, as shown in Figure 1, presenting a side view of the TiO_2 film under $100\times$ magnification. Figure 2 shows a top view of the TiO_2 film under $40\times$ magnification. The sintered films were then dyed using the extracts of natural dyes for 16 h under dark. The dyed TiO_2 electrode and a counter electrode fabricated from FTO-coated glass, with a sputtered layer of platinum catalyst, were assembled to form a solar cell by sandwiching a redox (I^-/I_3^-) electrolyte solution. The electrolyte solution is composed of 2 mL of acetonitrile, 8 mL of propylene carbonate (p-carbonate), 0.668 g of KI, and 0.0634 g of I_2 . Figure 3 shows a schematic diagram of the assembled DSSC and thickness of the TiO_2 layer.

2.3. Electrochemical impedance spectroscopy

Electrochemical IS measurements were performed using an Autolab instrument in combination with a frequency response analyzer (FRA). In a typical electrochemical impedance measurement, the FRA module generates a sine wave with a user-defined frequency and small amplitude. This signal is superimposed on the applied DC potential or current in the cell. The AC voltage and current components are analyzed by the 2 FRA channels and the transfer function. The total impedance (Z) is calculated together with the phase angle shift and the real and imaginary components of the total impedance. Electrochemical IS was measured for 3 cells using an Autolab instrument. After analyzing the results, the equivalent circuit for each cell was found. These cells were

prepared using dyes derived from berry, Mirabelle plum, and peach. The AC amplitude was set to 10 mV for all measurements. All measurements were carried out with NOVA software. The impedance was measured and plotted to obtain Nyquist and Bode plots.

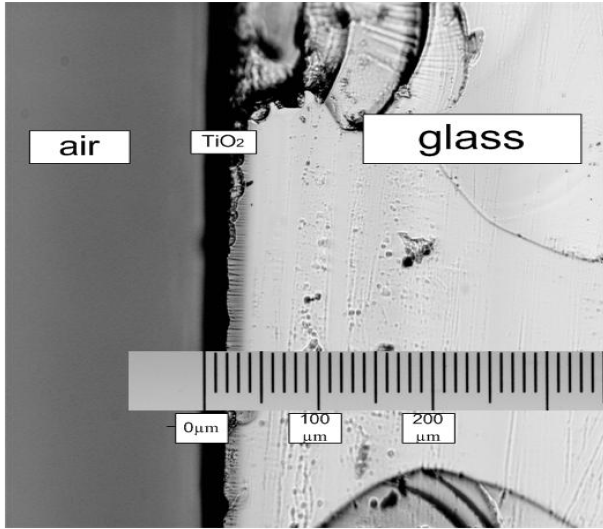


Figure 1. A side view of the TiO_2 film under $100 \times$ magnification.

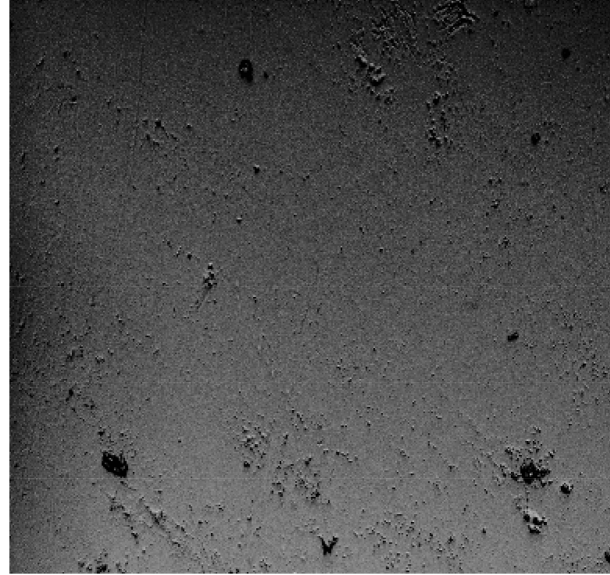


Figure 2. A top view of the TiO_2 film under $40 \times$ magnification.

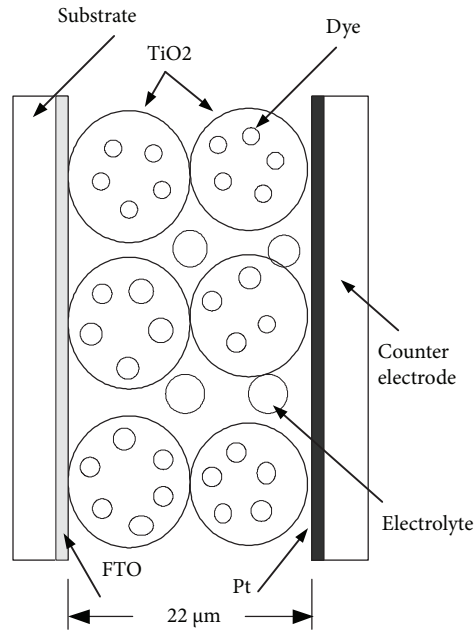


Figure 3. A schematic diagram showing the structure of the DSSC and the thickness of the semiconductor layer.

2.4. Measurements and results

The absorption spectra of the extracted pigments in ethyl alcohol solution were obtained using a UV-Vis spectrophotometer (Thermoline Genesys 6). The wavelength range of absorption spectra analysis extends from

350 to 800 nm. The J–V characteristic curves under illumination were obtained using a National Instruments data acquisition card (USB NI 6251) in combination with the LabVIEW program. The J–V curves were measured at 100 mW/cm^2 illumination using a high-pressure mercury arc lamp equipped with a band-pass IR filter to avoid heating the sample.

2.5. Absorption of natural dyes

The UV-Vis absorption spectra for the extracts from the leaves of plant cream, apricot, fig, apple, sage, thyme, mint, *Ziziphus jujuba*, orange, shade tree, basil, berries, Mirabelle plum, Victoria plum, peach, mango, pomegranate, banana, guava, and fluoridation-treated plant were investigated. Figure 4 shows the UV-Vis absorption spectra of 3 extracts dissolved in ethyl alcohol. As can be seen from Figure 4, there were absorption bands at about 415 nm and 664 nm for the extract of cream. The extract of apricot exhibited an absorption band at about 394 nm and 3 small bands at 506 nm, 535 nm, and 665 nm. The extract of fig showed absorption bands at about 413 nm and 663 nm. Generally, it was found that most of the dyes had absorption bands at about 400 nm and 667 nm. This is due to the fact that all samples were plant leaves, where chlorophyll is a major pigment.

2.6. Photoelectrochemical properties

The performance of natural dyes as DSSC sensitizers was evaluated by J_{sc} , V_{oc} , fill factor (FF), and energy conversion efficiency (η). Figure 5 shows the J–V curves of the DSSCs fabricated using the sensitizers extracted from 3 dyes. The DSSC output power was calculated as $P = JV$ using the J–V data. The maximum power (P_{max}) of each cell is then obtained. The current (I_{mp}) and the voltage (V_{mp}) corresponding to the maximum power point are then obtained. All the photoelectrochemical parameters of the DSSCs sensitized with different natural dyes are listed in Table 1. As displayed in Table 1, J_{sc} varied from 0.771 to 5.164 mA/cm^2 , V_{oc} changed from 0.573 to 0.703 V, and the FF of the fabricated DSSC ranged between 32.3% and 55.1%. The best performance was obtained from the DSSC sensitized by the *Ziziphus jujuba*, where the efficiency of the cell reached 1.077%. These results are similar to those of the DSSCs sensitized by other natural dyes in previous works [10–13].

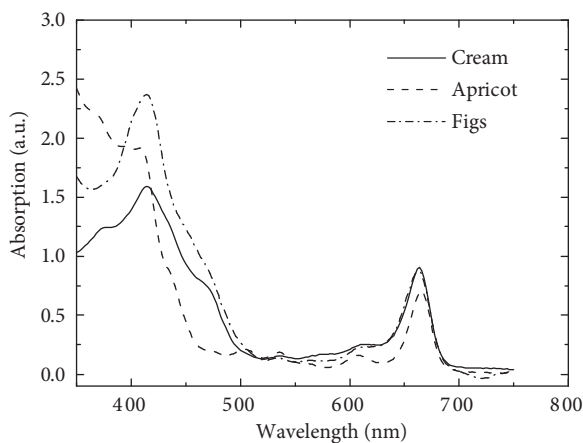


Figure 4. Absorption spectra of the extracts of cream, apricot, and fig using ethyl alcohol as a solvent.

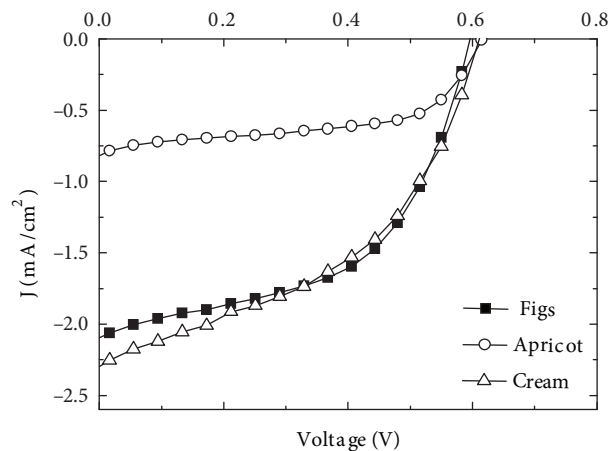


Figure 5. Current density–voltage characteristic curves for the DSSCs sensitized by cream, apricot, and fig.

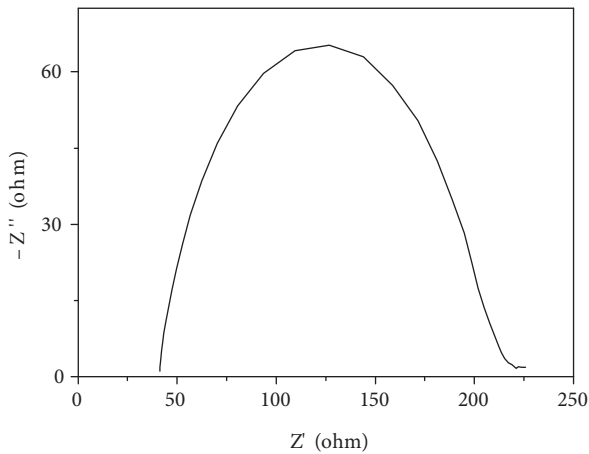
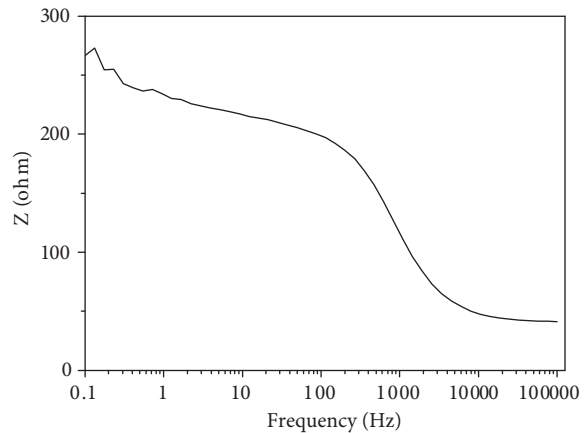
Table 1. Photovoltaic parameters of the fabricated DSSCs

Extract	J_{sc} (mA/cm ²)	V_{oc} (V)	J_m (mA/cm ²)	V_m (V)	FF	η (%)
Cream	2.281	0.610	1.451	0.421	0.440	0.607
Apricot	0.771	0.620	0.561	0.470	0.551	0.261
Fig	2.091	0.596	1.500	0.438	0.515	0.642
Apple	2.750	0.641	1.750	0.421	0.412	0.420
Sage	1.301	0.607	0.865	0.433	0.471	0.372
Thyme	0.712	0.596	0.444	0.425	0.440	0.187
Mint	0.980	0.579	0.487	0.387	0.400	0.227
<i>Ziziphus jujuba</i>	3.180	0.652	2.305	0.470	0.519	1.077
Orange	1.745	0.660	1.147	0.460	0.448	0.517
Shade tree	0.801	0.578	0.423	0.386	0.350	0.162
Basil	1.398	0.581	0.950	0.431	0.499	0.409
Berry	3.573	0.595	2.285	0.411	0.441	0.939
Mirabelle plum	5.164	0.573	2.877	0.330	0.323	0.958
Victoria plum	1.383	0.687	0.981	0.515	0.527	0.501
Peach	2.555	0.611	1.675	0.395	0.422	0.659
Mango	1.037	0.570	0.696	0.391	0.455	0.269
Pomegranate	0.907	0.581	0.514	0.391	0.379	0.200
Banana	1.770	0.596	1.214	0.429	0.492	0.522
Guava	2.130	0.582	1.243	0.400	0.401	0.498
Fluoridation-treated	2.474	0.703	1.731	0.483	0.480	0.835

2.7. Impedance spectroscopy

Electrochemical IS was used for DSSCs sensitized with berry, Mirabelle plum, and peach cells using an Autolab instrument. FRA potentiostatic scans have 3 types: FRA frequency scan, electrochemical circle fit, and fit and simulation data. The FRA frequency scan has 3 curves: Nyquist $-Z''$ vs Z' , Bode modulus, and Bode phase. Figures 6, 7, and 8 represent Nyquist, Bode modulus, and Bode phase curves, respectively, for the DSSC sensitized with berry. Figure 9 shows the equivalent circuit for the DSSC sensitized with berry.

The electronic resistance (R_s), charge-transfer resistance (R_P), and capacitance (C) are given in Figure 8.

**Figure 6.** Nyquist curve for the DSSC sensitized by berry.**Figure 7.** Bode modulus for the DSSC sensitized by berry.

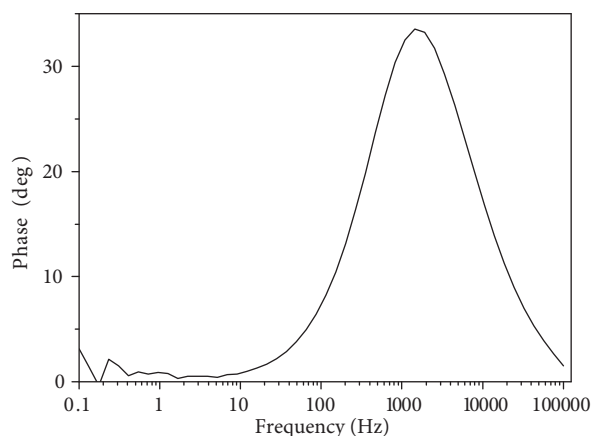


Figure 8. Bode phase curve for the DSSC sensitized by berry.

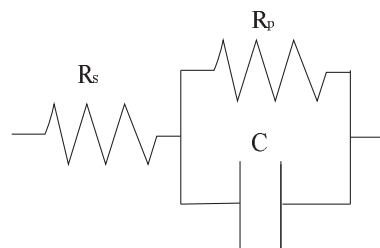


Figure 9. The equivalent circuit for a DSSC.

The low values of J_{sc} in the fabricated cells may be attributed to the fast charge recombination rate, loss resulting from various competitive processes, or incompatibility between the energy of the excited state of the adsorbed dye and the conduction band edge of TiO_2 . Moreover, the ground state of dye molecules could be considerably shifted with respect to the redox potential of I^-/I_3^- . On the other hand, low FF arises from the large series resistance and the low shunt resistance in the cells, as presented in Table 2. Series resistance arises from ohmic resistance, poor connection between material interfaces, or low mobility of the electrolyte. Low shunt resistance indicates that the current has alternative ways of crossing the cell other than the desired one, e.g., if the TiO_2 electrode is in almost direct contact with the counter electrode. In addition, the low response exhibited by the fabricated DSSCs may be due to the weak bonding between the dye molecule and TiO_2 film. Although chlorophyll plays a key role in photosynthesis in plants, this property cannot result in good photo-to-electric conversion in DSSCs because of the weak bonds between the dye molecules and TiO_2 films, through which electrons can be transported from an excited dye molecule to the TiO_2 film. Obviously, in photosensitization, the interaction and bonding between the dye and the TiO_2 film are very important in enhancing the photoelectric conversion efficiency of DSSCs.

Table 2. Values of the equivalent circuit elements for the 3 cells.

Extract	R_S (Ω)	R_P (Ω)	C (μF)
Berry	40.9	170	1.44
Mirabelle plum	33.3	815	2.50
Peach	48.6	451	1.51

Cells based on natural dyes appear to have low V_{oc} and J_{sc} , probably due to several complicated factors. Finding different additives for improving V_{oc} and J_{sc} might result in higher conversion efficiencies. Although the efficiencies obtained with these natural dyes are still below the current requirement for large-scale practical application, the results are encouraging and may boost additional studies of new natural sensitizers and optimization of solar cell components compatible with such dyes. Both the preparation of the nanocrystalline TiO_2 layer and the nature of redoxing electrolytes must be optimized to enhance cell efficiency.

3. Conclusion

In this paper, DSSCs were assembled using extracts from 20 plant leaves as sensitizers for nanocrystalline TiO₂ photoelectrodes. Photovoltaic parameters of the fabricated DSSCs were determined under 100 mW/cm² illumination. The best performance was obtained for the DSSC sensitized with the *Ziziphus jujuba*, where the efficiency of the cell reached 1.077%. The impedance spectroscopy of 3 cells was measured and the equivalent circuit was found.

References

- [1] O'Regan, B.; Gratzel, M. *Nature* **1991**, *353*, 737–740.
- [2] Hagfeldt, A.; Grätzel, M. *Acc. Chem. Res.* **2000**, *33*, 269–277.
- [3] Smestad, G.; Bignozzi, C.; Argazzi, R. *Sol. Energ. Mat. Sol. C* **1994**, *32*, 259–272.
- [4] Kim, S. S.; Yum, J. H.; Sung, Y. E. *Sol. Energ. Mat. Sol. C* **2003**, *79*, 495–505.
- [5] Calogero, G.; Di Marco, G. *Sol. Energ. Mat. Sol. C* **2008**, *92*, 1341–1346.
- [6] Luo, P.; Niu, H.; Zheng, G.; Bai, X.; Zhang, M.; Wang, W. *Spectrochim. Acta A* **2009**, *74*, 936–942.
- [7] Zhou, H.; Wu, L.; Gao Y.; Ma, T. *J. Photoch. Photobio. A* **2001**, *219*, 188–194.
- [8] Gómez-Ortíz, N. M.; Vázquez-Maldonado, I. A.; Pérez-Espadas, A. R.; Mena-Rejón, G. J.; Azamar-Barrios, J. A.; Oskam, G. *Sol. Energ. Mat. Sol. C* **2010**, *94*, 40–44.
- [9] El-Agez, T. M.; El Tayyan, A. A.; Al-Kahlout, A.; Taya, S. A.; Abdel-Latif, M. S. *Int. J. Mater. Chem.* **2012**, *2*, 105–110.
- [10] Taya, S. A.; El-Agez, T. M.; El-Ghamri, H. S.; Abdel-Latif M. S. *International Journal of Materials Science and Applications* **2013**, *2*, 37–42.
- [11] Polo, A. S.; Iha N. Y. M. *Sol. Energ. Mat. Sol. C* **2006**, *90*, 1936–1944.
- [12] Hao, S.; Wu, J.; Huang, Y.; Lin, J. *Sol. Energy* **2006**, *80*, 209–214.
- [13] Abdel-Latif, M. S.; El-Agez, T. M.; Taya, S. A.; Batniji, A. Y.; El-Ghamri H. S. *Materials Sciences and Applications* **2013**, *4*, 516–520.